JPE 19-6-20

https://doi.org/10.6113/JPE.2019.19.6.1544
ISSN(Print): 1598-2092 / ISSN(Online): 2093-4718

Regulated Incremental Conductance (r-INC) MPPT Algorithm for Photovoltaic Systems

Thusitha Randima Wellawatta* and Sung-Jin Choi†

†,*School of Electrical Engineering, University of Ulsan, Ulsan, Korea

Abstract

The efficiency of photovoltaic generation systems depends on the maximum power point tracking (MPPT) technique. Among the various schemes presented in the literature, the incremental conductance (INC) method is one of the most frequently used due to its superb tracking ability under changes in insolation and temperature. Generally, conventional INC algorithms implement a simple duty-cycle updating rule that is mainly found on the polarity of the peak-power evaluation function. However, this fails to maximize the performance in both steady-state and transient conditions. In order to overcome this limitation, a novel regulated INC (r-INC) method is proposed in this paper. Like the compensators in automatic control systems, this method applies a digital compensator to evaluate the INC function and improve the capability of power tracking. Precise modeling of a new MPPT system is also presented in the optimized design process. A 120W boost peak power tracker is utilized to obtain comparative test results and to confirm the superiority of the proposed method over existing techniques.

Key words: Linear feedback control systems, Maximum power point trackers, Photovoltaic systems, Solar power generation

I. INTRODUCTION

Photovoltaic (PV) generation systems play an important role in the production of green energy. The fact that PV systems do not produce acoustic noise, contribute to environmental pollution or emit any particles makes them a desirable target for study. In order to maximize solar energy utilization, the use of a maximum power point tracking (MPPT) technique is compulsory. The basic configuration of an MPPT system for a PV system is shown in Fig. 1, where the DC/DC converter includes an MPPT algorithm to control both the current and voltage for maximizing the extraction of energy from solar modules.

Among the many MPPT algorithms in the literature, the perturb and observation (P&O) and incremental conductance (INC) methods are the most widely used, due to their simple mathematical implementation [1]. However, these algorithms usually require a trade-off between the steady-state behavior and speed. The P&O algorithm responds quickly to changes in maximum power point (MPP). However, fluctuations around the MPP result in overall efficiency drops of the system [1], [2]. On the other hand, the INC method can eliminate such fluctuations at the cost of a lowered response speed [2]. In addition, there is also less misperception in the tracking direction [3].

Typically, peak-power evaluation function based "k" operation is used in the conventional INC, which reaches zero when the operating point reaches the exact MPP. Duty-cycle updating is done based on the sign of the k value as shown in (1).

$$d[n] = d[n-1] - sign(k)\delta \quad (1)$$

where δ represents a specific fixed step size of the duty change, and $d[n]$ is the quantized duty-cycle of the maximum power point tracker. However, as mentioned before, the conventional INC and the P&O method both o environment [2], [4]. To addres s this issue, different kinds of modified INC approaches have been developed. One such example is variable-step INC, where different sets of duty cycle update equations can be switched according to the distance between the current operating point and the MPP [4]-[11], where the value of δ in (2) varies according to the situation. Although such a modification improves the power tracking performance of the technique, it does not include any procedure to determine algorithm parameters (such as step size) without trial and

Manuscript received Jan. 24, 2019; accepted May 29, 2019
Recommended for publication by Associate Editor Younghoon Cho.
†Corresponding Author: sjchoi@ulsan.ac.kr
Tel: +82-52-259-1642, Fax: +82-52-259-1687, University of Ulsan
*School of Electrical Eng., University of Ulsan, Korea

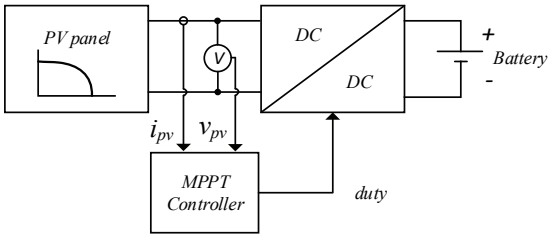

Fig. 1. Typical MPPT system with a battery load.

error. Furthermore, most variable-step INC methods have a complex algorithm flow. Other conventional methods such as hill climbing, predictive and numerical controlling, as well as different modified INCs have been proposed in the literature [12]-[17]. However, these methods are still hampered by implementation complexity due in part to the lack of a design procedure. In order to mitigate the above limitations, a novel regulated INC (r-INC) method was proposed in [19]. Like the compensator in automatic control system, this method utilizes the delayed error information of the evaluation function and enhances the power tracking capability. A systematic design procedure for determining the algorithm parameters is also presented with mathematical modeling and controller design. In this extended version, experimental waveforms according to an EN standard PV test scenario and more detailed performance evaluation have been provided, which clearly elaborates on the proposed method.

II. Proposed Method

The INC function, $k(V_{pv},I_{pv})$, is defined as a criterion to determine the status of MPP tracking. The value of k is defined in (2).

$$\frac{dp_{pv}}{dv_{pv}} = i_{pv} + v_{pv}\frac{di_{pv}}{dv_{pv}} \Rightarrow k(v_{pv}, i_{pv}) = \frac{i_{pv}}{v_{pv}} + \frac{\Delta i_{pv}}{\Delta v_{pv}} \quad (2)$$

Here p_{pv}, i_{pv} and v_{pv} are the output power, the output current and the terminal voltage of the PV module, respectively. By mathematical formulation, the smaller the value becomes, the closer the operating point approaches the maximum power point. At the MPP, the INC function should be zero. In the proposed scheme, each evaluation of $k(V_{pv},I_{pv})$ in the current operating point is compared with the reference value k_{ref} to obtain an error signal (3). In addition, a control loop steers the operating point to minimize the error. If the reference is chosen as zero, the operating point eventually approaches the maximum power point. According to the error information, the duty cycle of the DC/DC converter is updated with a digital filter as in (4).

$$e[n] = k_{ref} - k(v_{pv}, i_{pv})[n] \quad (3)$$

$$d[n] = b_0 e[n] + b_1 e[n-1] + b_2 e[n-2] - a_1 d[n-1], \quad (4)$$

where b_0, b_1, b_2 and a_1 are the filter coefficients noted in Table I, and n is the sequence number. Like a compensator in an automatic control system, a well-designed digital filter can enhance both the speed and stability of the power tracking capability. A flow chart of the r-INC algorithm is shown in Fig. 2.

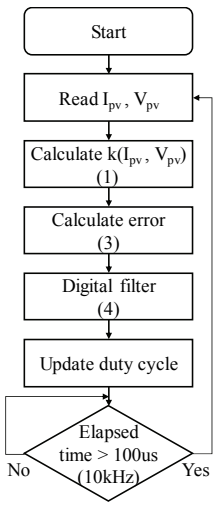

Fig. 2. Flow chart of the proposed INC algorithm.

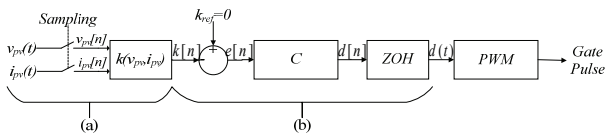

Fig. 3. Block diagram of the proposed algorithm.

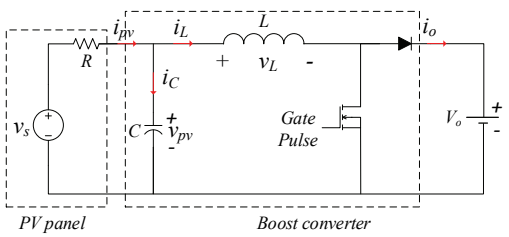

Fig. 4. Power stage.

A block diagram of the proposed method is shown in Fig. 3. In stage (a), the evaluation function is calculated by measuring v_{pv} and i_{pv}. In stage (b), the error is calculated by the mixer, and the duty information is determined by using the digital filter block. When k_{ref} = 0, the digital filter inevitably changes the duty cycle to regulate the value of k to zero, and to approach the operating point on the MPP. All of the blocks will then be examined and optimized, according to the control system concept outlined in the next section.

A typical power stage of a peak power tracker is shown in Fig. 4. Here, a boost converter under the CCM is used as an example. The battery is replaced by a constant voltage load and the PV module is modeled as a Thevenin equivalent circuit. The power stage transfer function $G_{id}(s)$ is used to represent the change in the PV current according to an ac disturbance in the duty cycle. The transfer function of the power stage (5) is determined by a small-signal analysis and a bode plot of the transfer function is shown in Fig. 5.

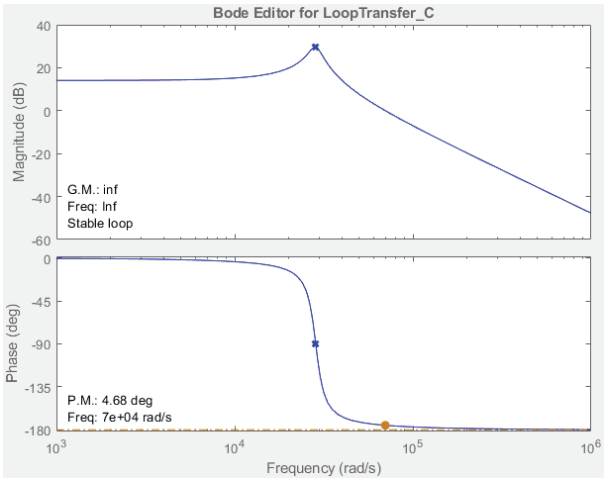

Fig. 5. Bode plot of the transfer function $G_{id}(s)$.

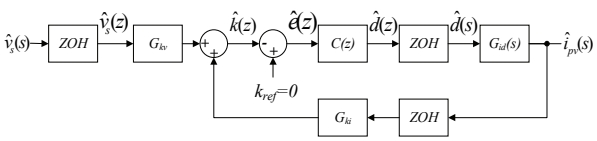

Fig. 6. Overall small signal block diagram.

$$G_{id} = \frac{\hat{i}_{pv}(s)}{\hat{d}(s)} = \frac{V_o}{R}\frac{1}{1+\frac{L}{R}s+LCs^2} \tag{5}$$

III. System Modelling and Design Procedure

The evaluation function of the peak-power k mentioned in (2) is a non-linear function controlled by the voltage and current of the PV system. Using the techniques in [18] and [19], the transfer gain for the MPP controller can be found by using the chain rules of partial derivation to (2) as follows:

$$G_{kv} = \frac{\hat{k}}{\hat{v}_s} = \frac{\partial k}{\partial v_{PV}}\frac{\partial v_{PV}}{\partial v_{PV}} = -I_{PV} \tag{6}$$

and:

$$G_{ki} = \frac{\hat{k}}{\hat{i}_{PV}} = \frac{\partial k}{\partial i_{PV}} = I_{PV}R + V_{pv} = V_S\,, \tag{7}$$

where G_{kv} and G_{ki} describe the incremental gain from both the voltage and the current to the k value, respectively. A small-signal block diagram of the overall MPPT system, including the power stage and the MPP controller, is shown in Fig. 6.

In order for the operating point to be positioned on the MPP, the system should eliminate any perturbations in the Thevenin equivalent voltage, v_s, of the PV modules. To accomplish this, an instantaneous change in the evaluation function (k) is compared with k_{ref} and the error signal is injected into the digital filter. A continuous duty-cycle is generated by the restructured duty signal $d[n]$. Through a

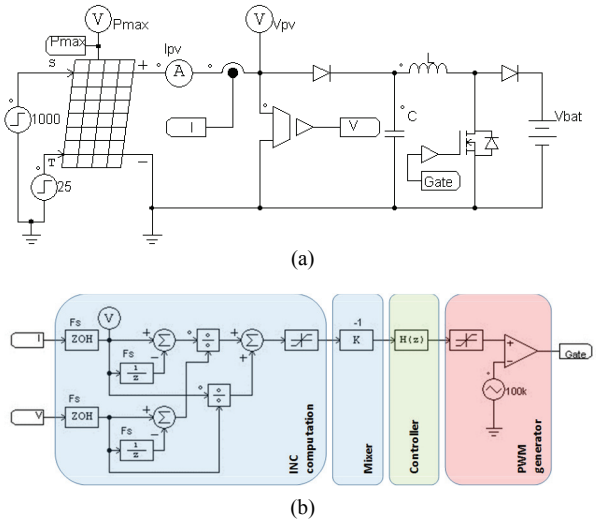

Fig. 7. PSIM simulation schematic. (a) Power stage. (b) Filter based INC MPPT system.

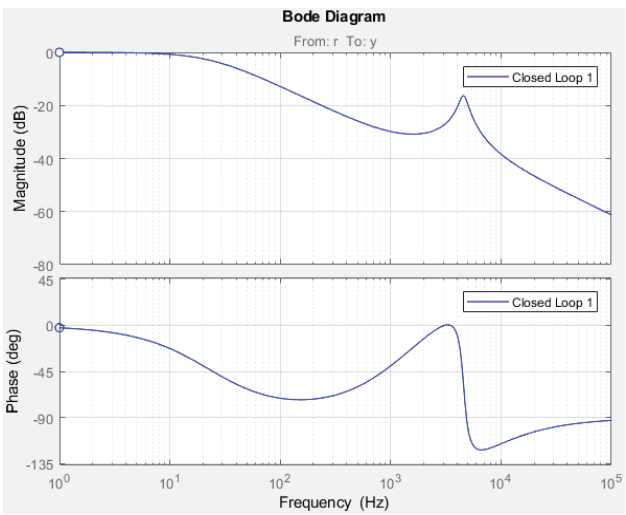

Fig. 8. Bode plot of the close loop transfer function ($G_{iv,close}$).

TABLE I
Simulation Parameters

Category	Parameter	Value
PV module BP MSX 120	P_{max}	120W
	V_{mpp}	33.7V
	I_{mpp}	3.56A
	V_{oc}	42.1V
	I_{sc}	3.87A
	Shunt res.	1000Ω
	Series res.	0.0015 Ω
Power circuit	C	22uF
	L	56uH
	V_o	48V
	f_{sw}	100kHz
Filter C(z)	f_s, f_{MPPT}	10kHz
	b_0	0.1541
	b_1	-0.1262
	b_2	0.0221
	a_1	-1

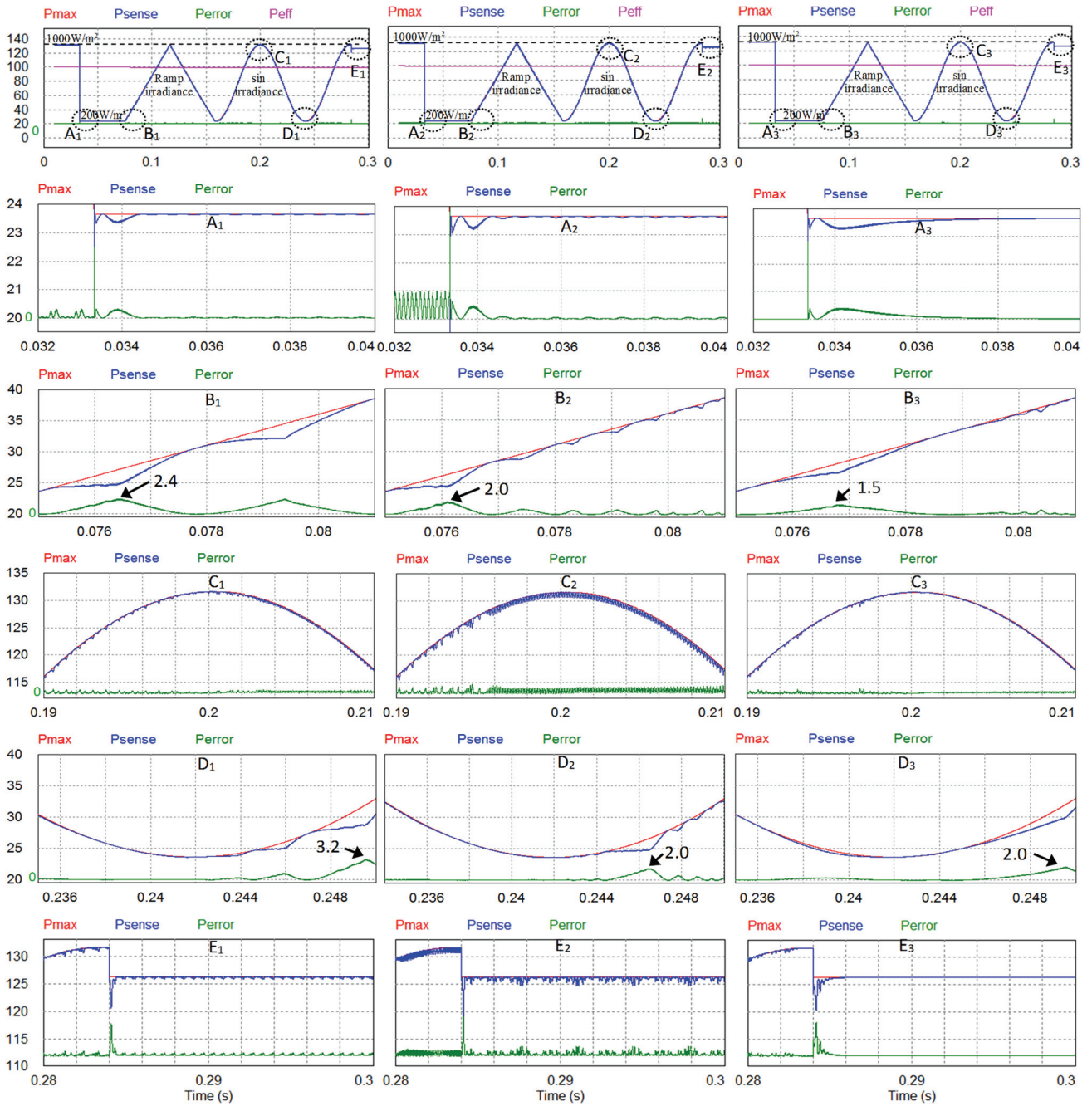

Fig. 9. Steady state and transient responses in the insolation change (A, B, C, D and E are magnifications of the main curve). (a) P&O. (b) Variable step INC. (c) Proposed INC.

control theory (such as block reduction techniques), the digital filter can be designed and used to maximize the performance of MPPT.

To verify the feasibility of the proposed scheme, a PSIM simulation is implemented as shown in Fig. 7. The PV module specification, the power stage, and filter parameters are shown in Table I. A 100kHz switching is used to minimize the size of the passive components, and the MPPT frequency is maintained at 10kHz [8] to avoid disturbances by noise [20]. After the analog PID filter C(s) has been constructed using MATLAB, the closed loop system can be derived as (8) and the bode plot is shown in Fig. 8.

$$G_{iv,close}(s)=\frac{\hat{i}_{pv}(s)}{\hat{v}(s)}\bigg|_{closed\_loop}=\frac{C(s)G_{id}(s)G_{ki}}{1+C(s)G_{id}(s)G_{ki}} \tag{8}$$

As a result, C(z) in (8) is transformed to be a z-transform function in (9) and its coefficients are shown in Table I.

$$C(z)=\frac{b_0+b_1z^{-1}+b_2z^{-2}}{1+a_1z^{-1}} \tag{9}$$

TABLE II
PERFORMANCE COMPARISONS IN SIMULATION TESTS

Condition	MPPT method	Undershoot (%P)	1% Settling time (s)	Avg. unrecoverable power at MPP (P_{error}) (W)	MPPT efficiency η (%)
1000→200W/m^2 20^{0}C Tm =0.3s	P&O	13.54	0.0009	0.1732	99.77
	Variable step INC	23.56	0.0007	0.2651	99.65
	Proposed INC	11.92	0.0013	0.1032	99.87

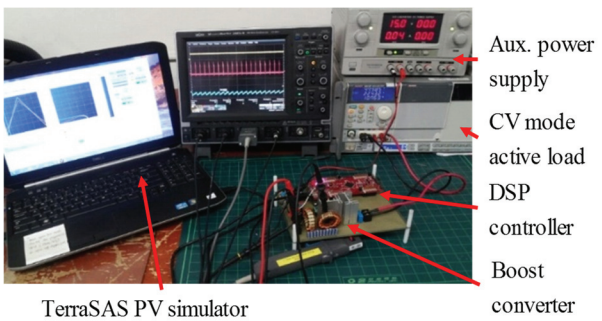

(a)

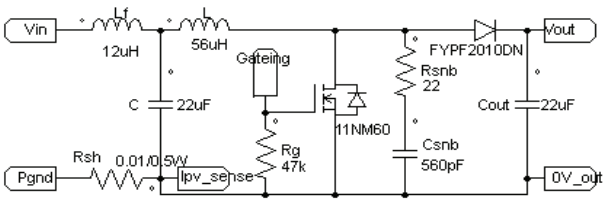

(b)

Fig. 10. Hardware setup and sch ematic for experiment. (a) Hardware setup. (b) Schematic for experiment.

IV. SIMULATION RESULTS

In order to verify the proposed MPPT algorithm, several performance indices have been calculated through simulation. The steady-state tracking performance was determined based on MPPT efficiency according to the EN50530 standard [21], and the transient responses was tested through a power output undershoot and a 1% settling time in response to step insolation changes. The proposed method was compared to the two previously discussed schemes (P&O and variable step INC) with the simulation results shown in Fig. 9. Note that all of the curves have been plotted as functions of power (W) vs. time (Sec). The simulations were performed between 200 and 1000W/m^2 insolation changes at 20^{0}C with 0.1msec sampling time. The MPPT efficiency was measured as a moving average using the formula in (A1) according to the EN50530, with the integration time in the efficiency formula being the same as the sampling time. In each graph, P_{max} denotes the maximum achievable output power from the PV module, and P_{sense} represents the instantaneous output power from the PV module. The MPPT accuracy is calculated as the percentage ratio of P_{sense} to P_{max}. The amount of unrecoverable power ($P_{max} - P_{sense}$) is indicated as P_{error}. Some critical changes in the simulation waveforms are magnified and marked as A, B, C and D in Fig. 9. Magnifications of the individual figures are made at the instants mentioned below:

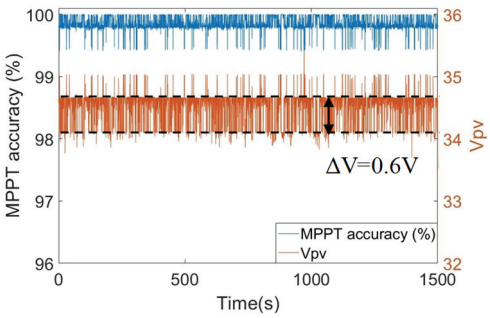

(a) P&O algorithm

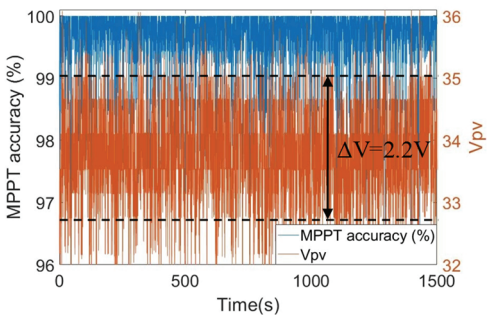

(b) V-INC algorithm

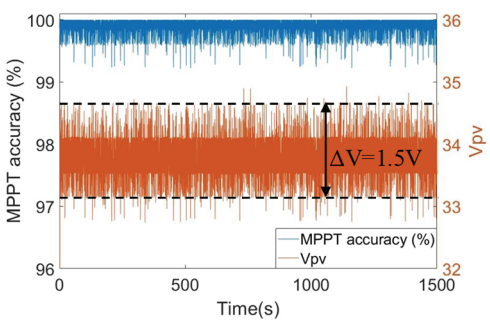

(c) r-INC algorithm

Fig. 11. Static MPPT hardware efficiency test 3. (a) P&O algorithm. (b) V-INC algorithm. (c) r-INC algorithm.

A – Step changes of the insolation (from 1000 to 200 W/m^2) under a constant temperature.

B – Constant insolation (200 W/m^2) starting to increase linearly.

C – Peak of the sinusoidal insolation (1000 W/m^2).

D – Minimum of the sinusoidal insolation (200 W/m^2).

E – Temperature step change (from 20 to 30^{0}C) under a 1000 W/m^2 constant insolation.

TABLE III
PERFORMANCE COMPARISONS IN HARDWARE EXPERIMENTS UNDER DYNAMIC PATTERNS

Condition	MPPT method	Max. power deviation (P_{error}) (W)	Avg. power loss at MPP (P_{error}) (W)	MPPT efficiency (η) (%)
Test B.1 (100→500W/m^2 25^{0}C) Tm =15936s	P&O	18.69	1.60	94.84
	Variable step INC	12.04	0.71	97.71
	Proposed INC	7.01	0.10	99.73
Test B.2 (300→1000W/m^2 25^{0}C) Tm =7000s	P&O	17.51	0.40	99.41
	Variable step INC	8.11	0.31	99.58
	Proposed INC	2.75	0.12	99.88
Test B.3 (10→100W/m^2 25^{0}C) Tm =17000s	P&O	2.03	0.79	89.38
	Variable step INC	2.77	0.67	91.36
	Proposed INC	0.83	0.14	98.25

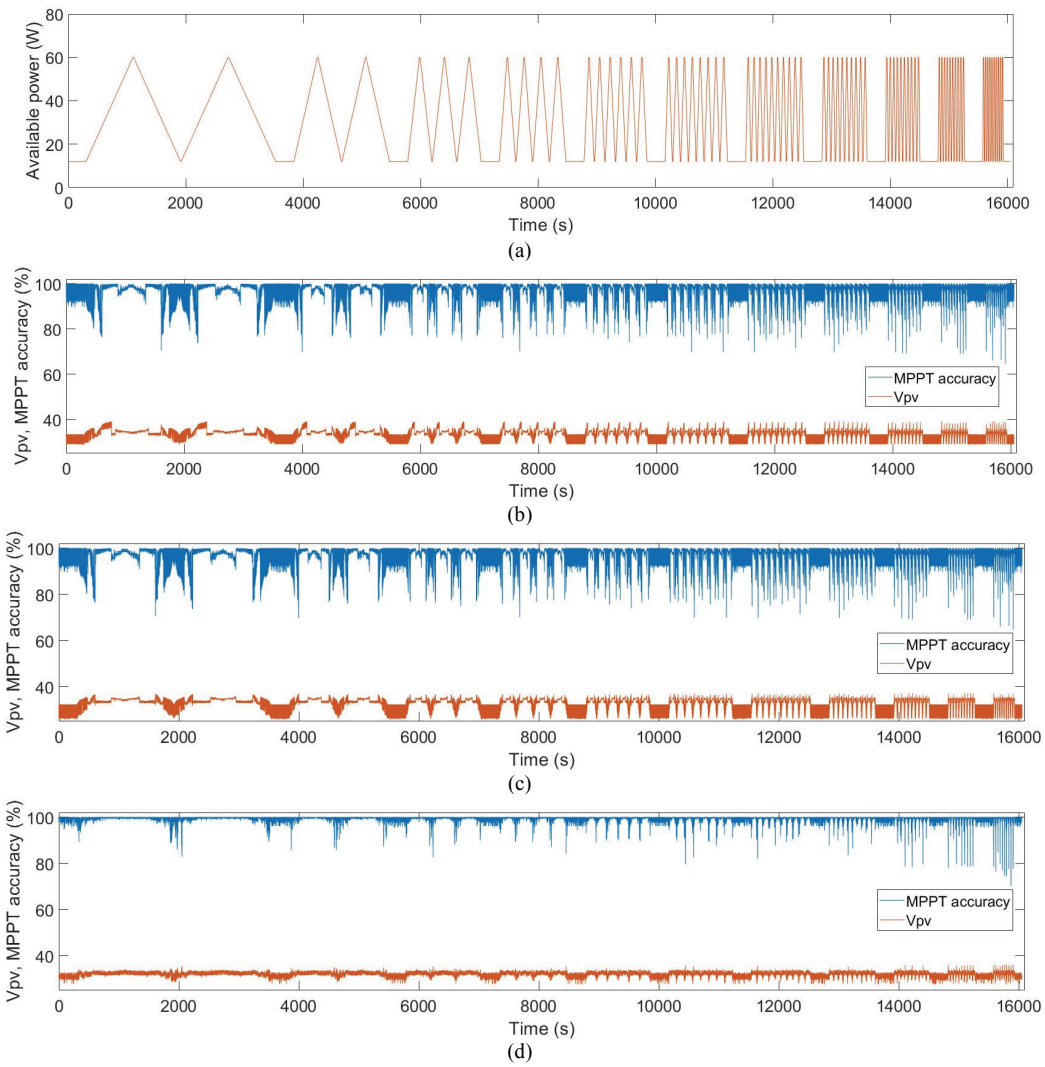

Fig. 12. Hardware test results (B-1 test sequence for functions of low and medium irradiance in the EN50530 standard). (a) MPP power. (b) MPPT accuracy of the P&O algorithm. (c) MPPT accuracy of the VINC algorithm. (d) MPPT accuracy of the r-INC algorithm.

In testing the conventional algorithms, the voltage perturbation size of the P&O was set to 0.006 V, and the duty-cycle resolution of the variable step INC was set to 0.01. In the simulation results, the undershoot and settling time were observed in 1000 to 200 W/m^2 step changes (magnification "A"). The average unrecoverable power in the MPP is obtained by averaging Perror, which represents the amount of unused or wasted power in the PV module.

TABLE IV
PERFORMANCE COMPARISONS OF HARDWARE EXPERIMENTS UNDER STATIC PATTERNS

Condition	MPPT method	Max. power deviation (W) (maximum P_{error})	Avg. unrecoverable power at MPP (W)	MPPT efficiency η (%)
(1000W/m^2 25^{0}C) Tm =1500s	P&O	1.36	0.20	99.83
	Variable step INC	7.55	0.41	99.65
	Proposed INC	0.96	0.14	99.88

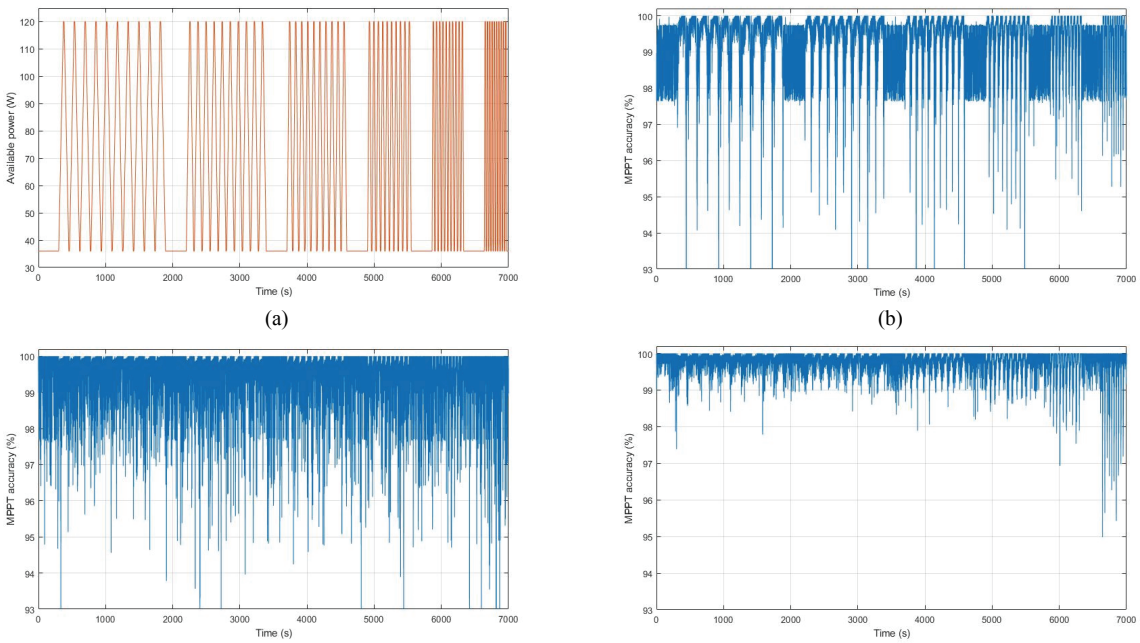

Fig. 13. Hardware test results (B-2 test sequence for functions of medium and high irradiance in the EN50530 standard). (a) MPP power. (b) MPPT accuracy of the P&O algorithm. (c) MPPT accuracy of the V-INC algorithm. (d) MPPT accuracy of the r-INC algorithm.

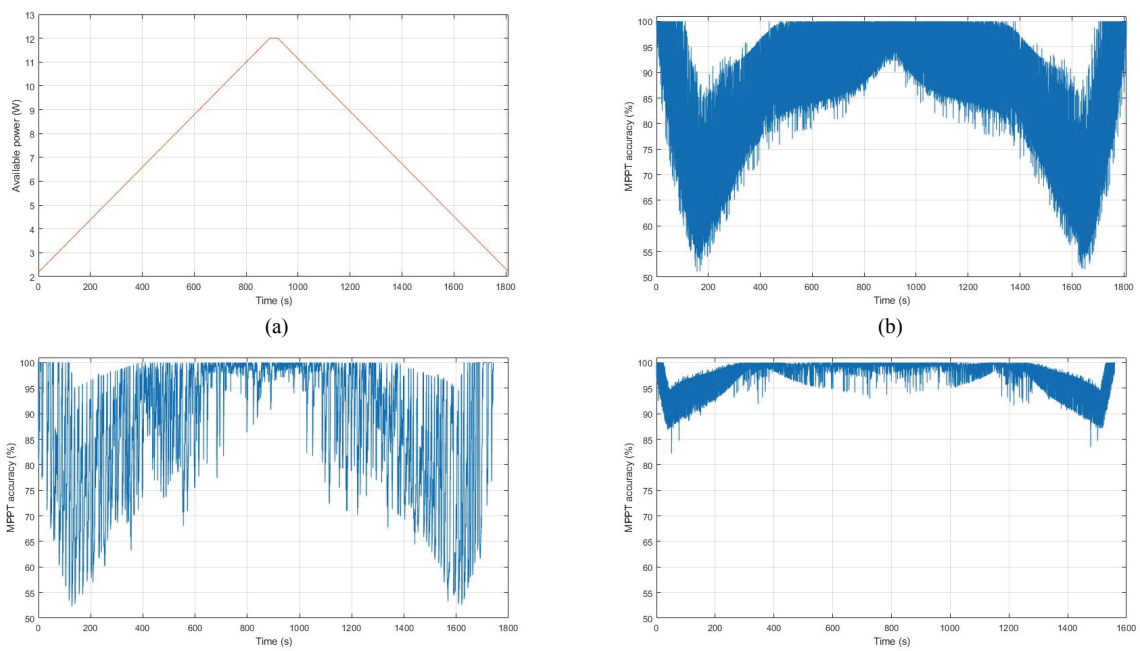

Fig. 14. Hardware test results (B-3 test sequence for the startup and shutdown in the EN50530 standard). (a) MPP power. (b) MPPT accuracy of the P&O algorithm. (c) MPPT accuracy of the V-INC algorithm. (d) MPPT accuracy of the r-INC algorithm.

Table V
Total MPPT Efficiency

MPPT method	Static MPPT efficiency(%)	Dynamic MPPT efficiency(%)
P&O	99.83	74.94
Variable step INC	99.65	96.21
Proposed INC	99.88	99.23

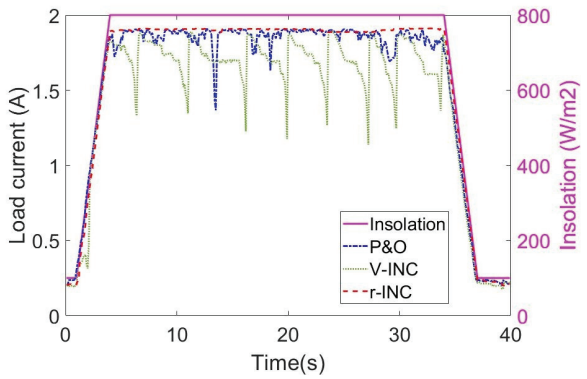

Fig. 15. Load current with the insolation profile.

V. Experimental Results

According to the results shown in Table II, the lowest undershoot is achieved with the novel proposed algorithm. Although the settling time becomes slightly longer, the power oscillation around the MPP is substantially reduced, which leads to improved efficiency. These results indicate that the proposed digitally compensated INC shows comparatively better performance than the conventional methods.

Fig. 10 shows an experimental setup of the proposed system. A PV simulator (TerraSAS) was used to generate various insolation and temperature profiles according to the EN50530 standard, and a DSP controller (F28377S) was used to implement the algorithms. The CV mode active load is used as the output load. Experiment tests were performed in two phases: a static test and a dynamic test, according to the EN50530 standard, with a sampling time of 0.1sec. The static MPPT efficiency was calculated through formula (A2) along with the two conventional methods: P&O and variable step INC (V-INC). Static MPPT efficiency test results are shown in Fig. 11 and Table IV. It is clear that the r-INC method shows the highest efficiency among the three methods, at 99.88%. Meanwhile, ΔV is highest in the V-INC method. It is smaller in the P&O and r-INC method.

Similarly, dynamic MPPT test patterns were injected and the resulting efficiency was calculated by formula (A3). These test results are shown in Figs. 12, 13 and 14, as well as Tables III, V and VI. The behavior of the load current with respect to the insolation is shown in Fig. 15. Under a constant voltage load, the load current follows the insolation profile. The total dynamic MPPT efficiency was calculated by formula (A4). The total dynamic MPPT efficiency is shown in Table V, where the proposed algorithm's 99.23% efficiency is 3% higher than the V-INC method and well above the efficiency of the P&O method.

VI. Conclusion

This paper presented a novel digital filter-based INC algorithm, where a digital filter automatically adjusts the duty cycle to regulate the evaluation function to zero and to make the operating point approach MPP. The new MPPT algorithm has been compared with the conventional P&O and INC methods in both simulation and hardware tests.

According to a comparison of the obtained results, the proposed method shows improved performance in terms of transient response as well as in steady state MPPT efficiency. Furthermore, through the mathematical modeling and design guidelines presented in this paper, all of the parameters in the proposed algorithm can be designed and implemented using classical filter design tools, which are well established and easily accessible for use by engineers.

Appendix

Efficiency calculation formulae according to the EN50530 standard [21].

A1. MPPT efficiency: MPPT efficiency is defined by the energy drawn by the device under test divided by the theoretical available energy in the MPP condition. It is given by:

$$\eta = \frac{\int_{T_m} P_{sense} dt}{\int_{T_m} P_{mpp} dt} f \qquad \text{(A1)}$$

where:

TM - measuring period.

PDC,t - instantaneous power value drawn by the device under test.

PMPP,t - instantaneous MPP power value provided by the PV simulator.

A2. Static MPPT efficiency: Static efficiency is the MPPT efficiency under a steady state insolation characteristic curve and is given by:

$$\eta_{MPPTstat} = \frac{1}{P_{MPP,PVS} \cdot T_M} \sum_i U_{DC,i} I_{DC,i} \Delta T \qquad \text{(A2)}$$

where:

Udc,i - sampled value of the inverter input voltage.

Idc,i - sampled value of the inverter input current.

T_M - overall measuring period.

ΔT - period between two subsequent sample values.

$P_{MPP,PVS}$ - MPP power provided by the PV simulator.

A3. Dynamic MPPT efficiency: Dynamic efficiency is the MPPT efficiency under a dynamic insolation characteristic curve and is given by:

$$\eta_{MPPTdyn} = \frac{1}{\sum_j P_{MPP,PVS,j}.\Delta T_j} \sum_i U_{DC,i} I_{DC,i} .\Delta T_i \qquad \text{(A3)}$$

where:

Udc,i - sampled value of the inverter input voltage.

Idc,i - sampled value of the inverter input current.

T_M - overall measuring period.

$P_{MPP,PVS}$ - MPP power provided by the PV simulator.

ΔT_j - period where the power $P_{MPP,PVS,j}$ provided.

ΔT_i - period where the powers Udc,i and Idc,i are sampled.

A4. Average dynamic MPPT efficiency: This is defined by the overall dynamic MPPT efficiency by averaging the B.1 test (test sequence for functions between low and medium insolation) and the B.2 test (test sequence for functions between medium and high insolation).

$$\eta_{MPPTdyn,t} = \frac{1}{N} \sum_{i=1}^{N} \eta_{MPPTdyn,i} \qquad \text{(A4)}$$

where:

$\eta_{MPPTdyn,t}$ - average dynamic MPPT efficiency.

$\eta_{MPPTdyn,i}$ - dynamic MPPT efficiency for each test.

N - number of test sequences.

ACKNOWLEDGMENT

This work was supported by the National Research Foundation of Korea (NRF) grant funded by the Korea government (MSIT) (No. 2017R1A2B4005488).

REFERENCES

[1] D. Sera, L. Mathe, T. Kerekes, S. V. Spataru, and R. Teodorescu, "On the perturb-and-observe and incremental conductance MPPT methods for PV systems," *IEEE J. Photovolt.*, Vol. 3, No. 3, pp. 1070-1078, Jul. 2013.

[2] N. E. Zakzouk, M. A. Elsaharty, A. K. Abdelsalam, A. A. Helal, and B. W. Williams, "Improved performance low-cost incremental conductance PV MPPT technique," *IET Renew. Power Gener.*, Vol. 10, No. 4, pp. 561-574, Apr. 2016.

[3] M.A. Elgendy, B. Zahawi, and D.J. Atkinson, "Assessment of the incremental conductance maximum power point tracking algorithm," *IEEE Trans. Sustain. Energy*, Vol. 4, No. 1, pp. 108-117, Jan. 2013.

[4] Y.T. Chen, Z.H. Lai, and R.H. Liang, "A novel auto-scaling variable step-size MPPT method for a PV system," *Solar Energy*, Vol.102, pp. 247-256, Jan. 2014.

[5] F. Liu, S. Duan, F. Liu, B. Liu, and Y. Kang, "A variable step size INC MPPT method for PV systems," *IEEE Trans. Ind. Electron*., Vol. 55, No. 7, pp.2622-2628, Jul. 2008.

[6] Y. Tian, B. Xia, Z. Xu, and W. Sun, "Modified asymmetrical variable step size incremental conductance maximum power point tracking method for photovoltaic systems," *J. Power Electron*., Vol. 14, No. 1, pp. 156-164, Jan. 2014.

[7] Q. Mei, M. Shan, L. Liu, and J. M. Guerrero, "A novel improved variable step-size incremental-resistance MPPT method for PV systems," *IEEE Trans. Ind. Electron*., Vol. 58, No. 6, pp. 2427-2434, Jun. 2011.

[8] M. Mosa, M. B. Shadmand, R. S. Balog, and H. A. Rub, "Efficient maximum power point tracking using model predictive control for photovoltaic systems under dynamic weather condition," *IET Renew. Power Gener.*, Vol. 11, No. 11, pp. 1401-1409, Sep. 2017.

[9] A. Tomar and S. Mishra, "Synthesis of a new DLMPPT technique with PLC for enhanced PV energy extraction under varying irradiance and load changing conditions," *IEEE J. Photovolt*., Vol. 7, No. 3, pp. 839-848, May 2017.

[10] A. Thangavelu, S. Vairakannu, and D. Parvathyshankar, "Linear open circuit voltage variable-step-size incremental conductance strategy-based hybrid MPPT controller for remote power applications," *IET Power Electron*., Vol. 10, No. 11, pp. 1363-1376, Sep. 2017.

[11] D.C. Huynh and M.W. Dunnigan, "Development and comparison of an improved incremental conductance algorithm for tracking the MPP of a solar PV panel," *IEEE Trans. Sustain. Energy*, Vol. 7, No. 4, pp. 1421-1429, Oct. 2016.

[12] A. A. Abdelmoaty, M. Al-Shyoukh, Y. C. Hsu, and A. A. Fayed, "A MPPT circuit with 25 μW power consumption and 99.7% tracking efficiency for PV systems," *IEEE Trans. Circuits and Syst. I*, Vol. 64, No. 2, pp. 272-282, Feb. 2017.

[13] V. N. Lal and S. N. Singh, "Modified particle swarm optimisation-based maximum power point tracking controller for single-stage utility-scale photovoltaic system with reactive power injection capability," *IET Renew. Power Gener.*, Vol. 10, No. 7, pp. 899-907, Jul. 2016.

[14] A. Belkaid, J. P. Gaubert, and A. Gherbi, "Design and implementation of a high-performance technique for tracking PV peak power," *IET Renew. Power Gener*., Vol. 11, No. 1, pp. 92-99, Apr. 2017.

[15] H. Taheri and S. Taheri, "Two-diode model-based nonlinear MPPT controller for PV systems," *Canadian J. Electr. and Comput. Eng.*, Vol. 40, No. 2, pp. 74-82, Aug. 2017.

[16] R.B.A. Koad, A.F. Zobaa, and A. El-Shahat, "A novel MPPT algorithm based on particle swarm optimization for photovoltaic systems," *IEEE Trans. Sustain. Energy*, Vol. 8, No. 2, pp. 468-476, Apr. 2017.

[17] N. Ghaffarzadeh and S. Bijani, "Dual surface sliding mode controller for photovoltaic systems enhanced by a ripple domain search maximum power point tracking algorithm for fast changing environmental conditions," *IET Renew. Power Gener.*, Vol. 10, No. 5, pp. 611-622, May 2016.

[18] E. M. Ahmed and M. Shoyama, "Stability study of variable step size incremental conductance/impedance MPPT for PV systems," *Proceedings of 8th International Conference on Power Electronics (ICPE 2011) - ECCE Asia*, 2011.

[19] T. R. Wellawatta, Y. T. Seo, H. H. Lee, and S. J. Choi, "A regulated incremental conductance (R-INC) MPPT algorithm for photovoltaic system," *2017 IEEE Energy Conversion Congress and Exposition (ECCE)*, pp. 2305-2309, 2017.

[20] M. A. Elgendy, D. J. Atkinson, and B. Zahawi, "Experimental investigation of the incremental conductance maximum power point tracking algorithm at high perturbation rates," *IET Renew. Power Gener*., Vol. 10, No. 2, pp. 133-139, Feb. 2016.

[21] EN 50530, Overall Efficiency of Grid Connected Photovoltaic Inverters, BSI, 2013.

Thusitha Randima Wellawatta was born in Colombo, Sri Lanka. He received his B.S. degree in Electrical Engineering from the Engineering Council, London, ENG, UK, in 2012. He is presently working towards his M.S. (leading to his Ph.D.) degree at the University of Ulsan, Ulsan, Korea. From 2010 to 2014, he worked as an Automation Engineer with API Technologies, Colombo, Sri Lanka. Since 2014, he has been working as an Assistant Researcher in the School of Electrical Engineering, University of Ulsan, Ulsan, Korea since 2014 and working toward the MS leading Ph.D. Degree. His current research interests include power electronics and control, which includ photovoltaic generation and utilization, maximum power point tracking algorithms, PV partial shading algorithms and solar array simulators.

Sung-Jin Choi received his B.S., M.S. and Ph.D. degrees in Electrical Engineering from Seoul National University, Seoul, Korea, in 1996, 1998 and 2006, respectively. From 2006 to 2008, he worked as a Research Engineer with Palabs Company, Ltd., Seoul, Korea. From 2008 to 2011, he was working as a Principal Research Engineer at Samsung Electronics Company, Ltd., Suwon, Korea, where he was developing LED drive circuits and wireless battery charging systems. In 2011, he joined the University of Ulsan, Ulsan, Korea, where he is presently working an Associate Professor in the School of Electrical Engineering. From 2017 to 2018, he was a Visiting Scholar at San Diego State University, San Diego, CA, USA. His current research interests include power processing technology related to solar power generation, battery management and wireless power transfer.